


Research Article

Epitope-Based Peptide Vaccine Design against Fructose Bisphosphate Aldolase of *Candida glabrata*: An Immunoinformatics Approach

Lina Mohamed Elamin Elhasan ¹, Mohamed B. Hassan ², Reham M. Elhassan ³,
Fatima A. Abdelrhman ⁴, Essam A. Salih ⁵, Asma Ibrahim H ⁶, Amna A. Mohamed ⁷,
Hozaifa S. Osman ², Marwa Saad M. Khalil ⁷, Athar A. Alsafi ¹, Abeer Babiker Idris ⁸,
and Mohamed A. Hassan ^{4,9}

¹Faculty of Science and Technology, Department of Biotechnology, Omdurman Islamic University, Khartoum, Sudan

²Faculty of Medicine and Health Science, Omdurman Islamic University, Khartoum, Sudan

³Department of Pharmaceutical Chemistry, Faculty of Pharmacy, Sudan International University, Khartoum, Sudan

⁴Department of Biotechnology, Africa City of Technology, Khartoum, Sudan

⁵Biology and Technology Department, College of Applied and Industrial Sciences, University of Bahri, Khartoum, Sudan

⁶Faculty of Pharmacy, National Ribat University, Khartoum, Sudan

⁷Al-Neelain Medical Research Center, Al-Neelain University, Khartoum, Sudan

⁸Department of Medical Microbiology, Faculty of Medical Laboratory Sciences, University of Khartoum, Khartoum, Sudan

⁹Department of Translation Bioinformatics, Detavax Biotech, Kayseri, Turkey

Correspondence should be addressed to Lina Mohamed Elamin Elhasan; lina2014371@gmail.com

Received 10 July 2020; Revised 27 March 2021; Accepted 12 April 2021; Published 5 May 2021

Academic Editor: Roberta Antonia Diotti

Copyright © 2021 Lina Mohamed Elamin Elhasan et al. This is an open access article distributed under the Creative Commons Attribution License, which permits unrestricted use, distribution, and reproduction in any medium, provided the original work is properly cited.

Background. *Candida glabrata* is a human opportunistic pathogen that can cause life-threatening systemic infections. Although there are multiple effective vaccines against fungal infections and some of these vaccines are engaged in different stages of clinical trials, none of them have yet been approved by the FDA. **Aim.** Using immunoinformatics approach to predict the most conserved and immunogenic B- and T-cell epitopes from the fructose bisphosphate aldolase (Fba1) protein of *C. glabrata*. **Material and Method.** 13 *C. glabrata* fructose bisphosphate aldolase protein sequences (361 amino acids) were retrieved from NCBI and presented in several tools on the IEDB server for prediction of the most promising epitopes. Homology modeling and molecular docking were performed. **Result.** The promising B-cell epitopes were AYFKEH, VDKEPLYTK, and HVDKESLYTK, while the promising peptides which have high affinity to MHC I binding were AVHEALAPI, KYFKRMAAM, QTSNGGAAY, RMAAMNQWL, and YFKEHGEPL. Two peptides, LFSSHMLDL and YIRSIAPAY, were noted to have the highest affinity to MHC class II that interact with 9 alleles. The molecular docking revealed that the epitopes QTSNGGAAY and LFSSHMLDL have the lowest binding energy to MHC molecules. **Conclusion.** The epitope-based vaccines predicted by using immunoinformatics tools have remarkable advantages over the conventional vaccines in that they are more specific, less time consuming, safe, less allergic, and more antigenic. Further in vivo and in vitro experiments are needed to prove the effectiveness of the best candidate's epitopes (QTSNGGAAY and LFSSHMLDL). To the best of our knowledge, this is the first study that has predicted B- and T-cell epitopes from the Fba1 protein by using in silico tools in order to design an effective epitope-based vaccine against *C. glabrata*.

1. Introduction

Candidiasis is a fungal infection that has a high burden of morbidity and mortality in hospitalized and immunocompromised patients. It occurs in more than a quarter of a million patients every year with incidence rates for candidemia of 2–14 per 100,000 [1–4]. In general, *Candida* species infection ranges from superficial mucosal candidiasis such as vulvovaginal candidiasis and oropharyngeal candidiasis to serious systemic infection such as candidemia or fungemia [5–8]. Pathogenicity is facilitated by a number of virulence factors, most importantly its ability to adhere to host surfaces including medical devices, biofilm formation, and secretion of hydrolytic enzymes. Also, *Candida* cells elaborate polysaccharides, proteases, phospholipases, and hemolysins that cause host cell damage which leads to the increase in the incidence and antifungal resistance of NCAC species, specifically *C. glabrata*, and the unfortunate high morbidity and mortality associated with these species [8, 9].

Candida glabrata (*C. glabrata*) is a human opportunistic pathogen that can cause life-threatening systemic infections. *C. glabrata* is not polymorphic, grows as blastoconidia (yeast), and lacks pseudohyphal formation, so it is classified in the genus *Torulopsis*. *C. glabrata* cells (1–4 μm in size) forms glistening, smooth, and cream-colored colonies [10, 11]. During the infection, *C. glabrata* pathogens invade the macrophages, which are considered part of the innate immune system which is the first line of defense against invading pathogens. *C. glabrata* is able to modify the macrophage's phagosomal compartment, avoiding full maturation and acidification, and thus prevents the forming of the phagolysosomal environment [12]. *C. glabrata* is able to invade the bloodstream and different organs in a mouse model that have intragastric infections [13].

C. glabrata has a haploid genome—published in 2004 by Dujon et al. [14]—that allows adaptation to a wide range of environments [9, 15, 16]. Also, its genome contains more tandem repeats of genes than the other *Nakaseomyces* [17] and covers 67 genes encoding putative adhesin (cell wall proteins), including the Epa family with 17 members [16, 18], such as epithelial adhesin 1 (Epa1p) [19] and fructose biphosphate aldolase protein (Fba1) which play an essential role in the pathogenicity of *Candida* species mainly in the adhesion of the pathogen to the host [20, 21].

Fba1 is a yeast cell wall protein which presents in multiple species of *Candida*, e.g., *C. glabrata*, *C. parapsilosis*, *C. tropicalis*, and *C. albicans* fungal pathogens [22–26]. Fba1 is an important enzyme in the glycolytic pathway [27–30] and is also a multifunctional protein [31] that can facilitate the attachment (adhesion) to human cells or abiotic surfaces [32–34], protects *Candida* cells from the host's immune system [33], and promotes the detoxification of the ROS generated during the respiratory burst [21, 33, 34]. However, proteomics analysis revealed that Fba1 is the most abundant and stable enzyme in *Candida*. Moreover, it is considered one of the main immunodominant proteins [35, 36] in *Candida* cells and has been tested in the murine model as a protected protein against *Candida* [37], especially *C. albicans*, and also introduced immunity to

C. glabrata [34]; therefore, Fba1 is a potential antifungal target in yeast [38]. Multiple vaccines used Fba1 as an immunogenic protein against different pathogens such as the lethal and challenging *S. pneumoniae*, *Salmonella* spp., and *M. bovis* [39, 40].

The incidence of fungal infection has been increasing in the last few years, due to several factors such as misuse of broad-spectrum antibiotics, cytotoxic chemotherapy, immunocompromised patients, and transplantations [15, 41]. Invasive fungal infections are a major cause of global morbidity and mortality, accounting for about 1.4 million deaths per year [42]. Systemic fungal infections cost the healthcare industry approximately \$2.6 billion per year in the USA alone [43]. However, *Candida* species pose a base problem in hospitals, according to Healthcare-Associated Infections (HAI) [19, 44–46]. Although there are multiple effective vaccines against fungal infections and some of these vaccines are engaged in different stages of clinical trials, none of them have yet been approved by the FDA [47]. Therefore, there is an urgent and crucial need to design vaccines against the *Candida* species that might improve the quality of life for immunosuppressed patients [48].

The aim of this study is to predict the most conserved and immunogenic B- and T-cell epitopes from the Fba1 protein of *C. glabrata* by using in silico tools with the immunoinformatics approach presented in the IEDB server [49, 50]. This approach has multiple benefits in comparison to other approaches by being affordable, safe, time-saving, and clinically applicable using different computational software techniques [51–53]. To the best of our knowledge, this is the first study that has predicted the best candidates of multiple epitopes for Fba1 protein against *C. glabrata*.

2. Materials and Methods

In this study, we have used a variety of bioinformatics databases and tools for the prediction of the most promising peptides, through three phases shown in Figure 1.

2.1. Retrieval of Fructose Biphosphate Aldolase Protein Sequences. 13 *Candida glabrata* fructose biphosphate aldolase protein sequences (361 amino acids) were retrieved from the NCBI (<https://www.ncbi.nlm.nih.gov/protein>) database on 21 January 2019. The accession numbers of fructose biphosphate aldolase protein sequences were CAG61849.1, XP_448879.1, KTB01194.1, KTB08502.1, KTB09791.1, KTB12564.1, KTB19354.1, KTB25695.1, KTB27082.1, OXB40821.1, OXB46121.1, SLM13767.1, and SCV14850.1 [20].

2.2. Determination of Conserved Regions. Multiple sequence alignment (MSA) was used to determine the conserved regions; the retrieved sequences were aligned by MSA using Clustal W as applied in the BioEdit [54].

2.3. Prediction of B-Cell Epitope. The reference sequence of fructose biphosphate aldolase protein was submitted to the following B-cell tests [49, 50].

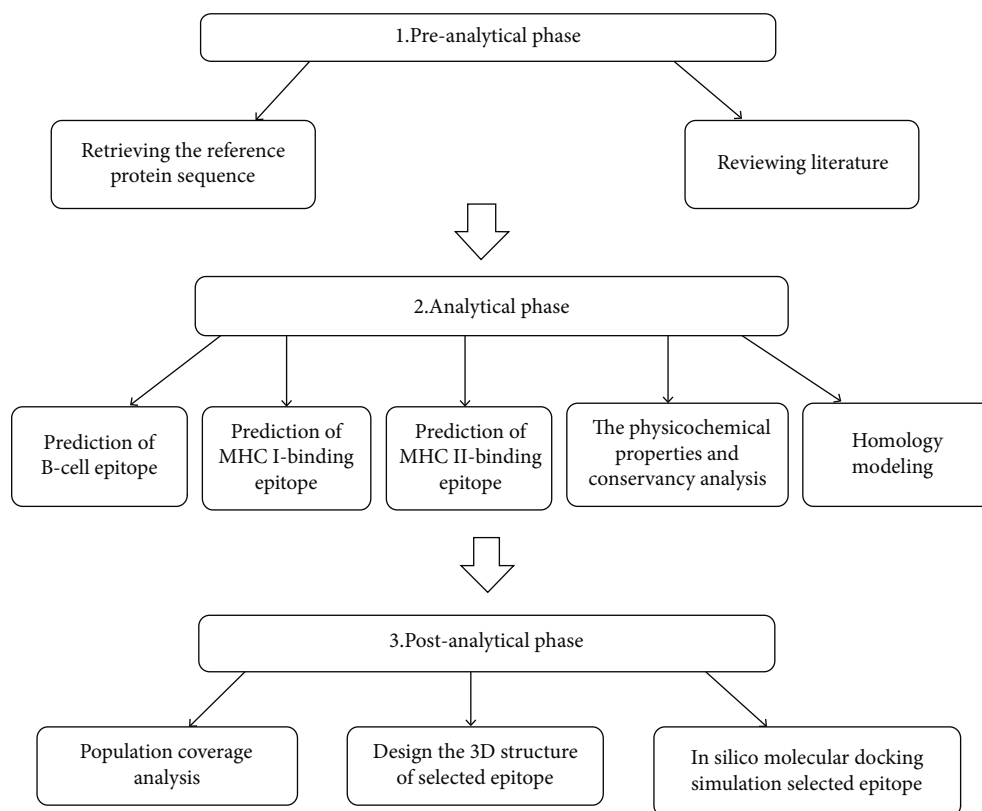


FIGURE 1: Schematic representation of the methodology phases.

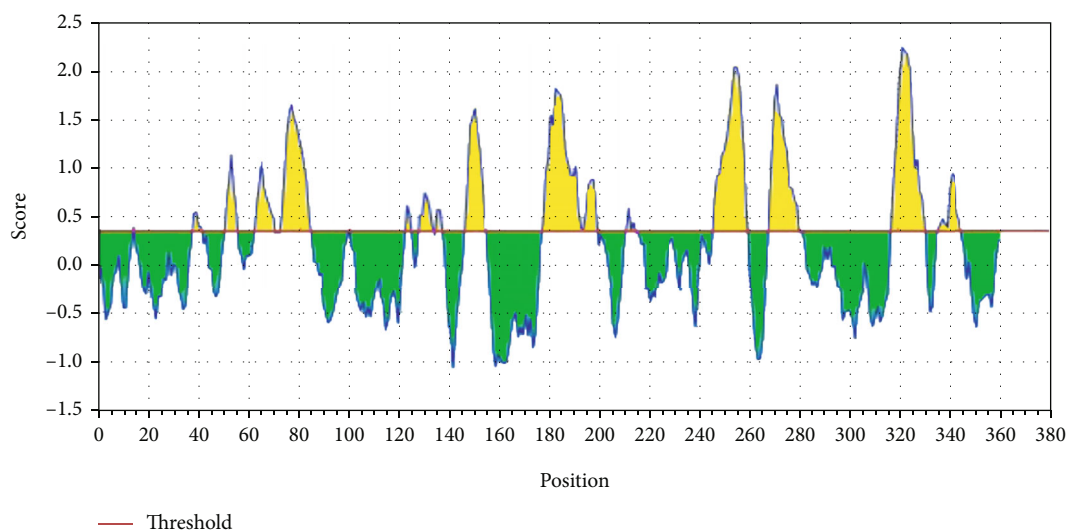


FIGURE 2: Bepipred linear epitope prediction: the red line is the threshold; above (the yellow part) is proposed to be part of the B-cell epitope.

2.3.1. Prediction of Linear B-Cell Epitopes. A collection of methods to predict linear B-cell epitopes based on protein sequence characteristics of the antigen using amino acid scales and HMMs was used.

The Bepipred tool from IEDB (<http://tools.iedb.org/bcell/result/>) was used to predict the linear B-cell epitopes

from the conserved region with a default threshold value of 0.350 [55–57].

2.3.2. Prediction of Surface Accessibility. Emini surface accessibility prediction tool of the Immune Epitope Database (IEDB) (<http://tools.iedb.org/bcell/result/>) was used to

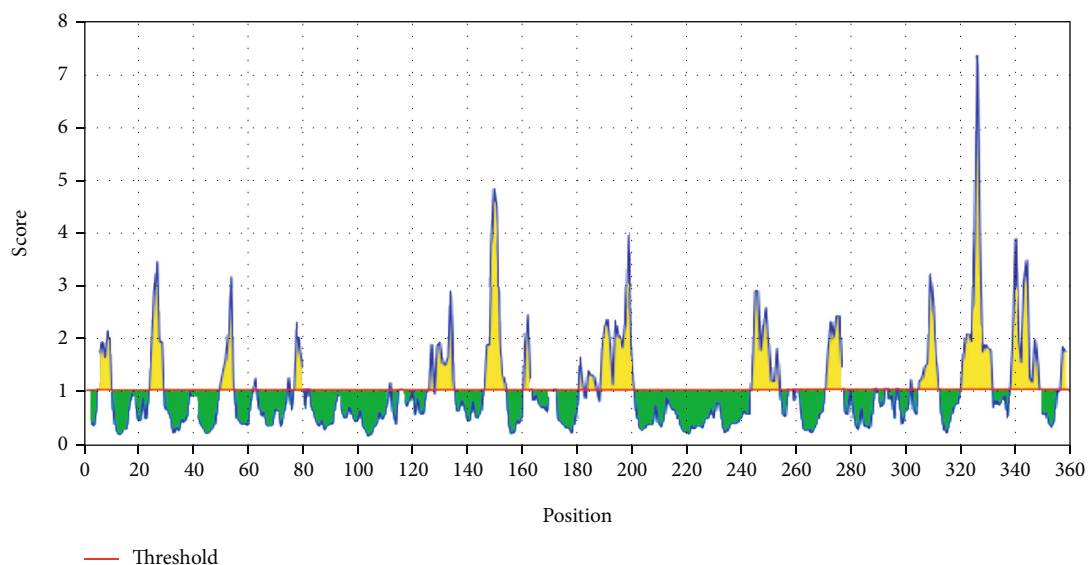


FIGURE 3: Emini's surface accessibility prediction test: the red line is the threshold; above (the yellow part) is proposed to be part of the B-cell epitope.

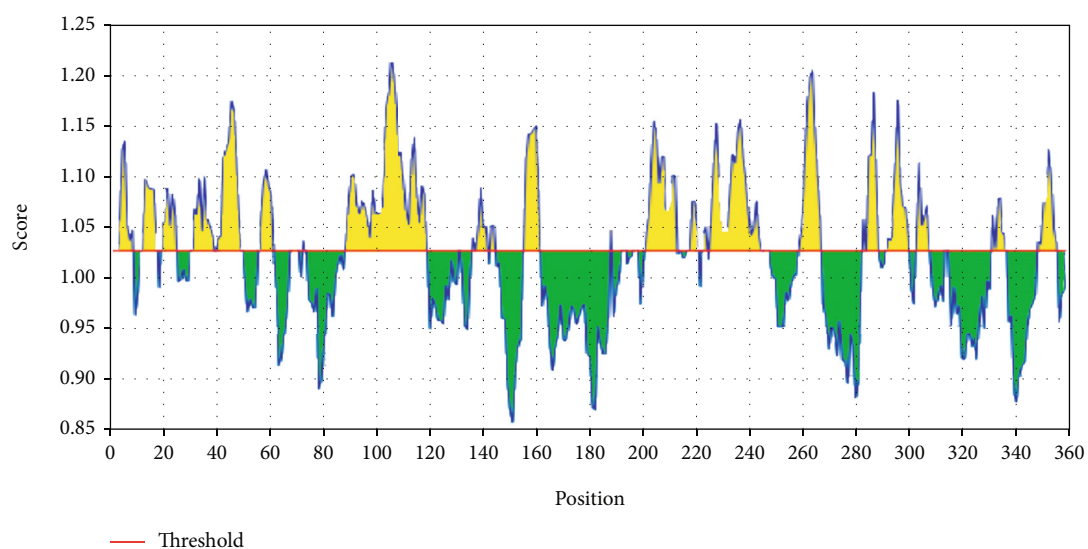


FIGURE 4: Kolaskar and Tongaonkar antigenicity prediction test: the red line is the threshold; above (the yellow part) is proposed to be part of the B-cell epitope.

TABLE 1: The proposed predicted antigenic B-cell epitopes; 9 antigenic sites were identified from fructose bisphosphate aldolase of *C. glabrata*.

Start	End	Peptide	Length
63	70	SNGGAAYF	8
73	84	KGVSNDGQNASI	12
129	134	AYFKEH	6
147	155	SEETDDENI	9
178	199	ITGGEEGDGVNNEHVDKESLYTK	22
247	260	KYAAEKTGAPAGSK	14
269	280	GSGSTQEEFNTG	12
318	331	GNPEGADKPNKKFF	14
336	345	WVREGEKTMS	10

to predict the surface epitopes from the conserved region with the default threshold value 1.0 [58].

2.3.3. Prediction of Epitope Antigenicity. The Kolaskar and Tongaonkar antigenicity method was used to detect the antigenic sites with a default threshold value of 1.025 (<http://tools.iedb.org/bcell/result/>) [59].

2.3.4. Prediction of Discontinuous B-Cell Epitopes. This method predicts epitopes based upon solvent-accessibility and flexibility. The methods are for modeling, docking of antibody, and protein 3D structures (<http://tools.iedb.org/bcell/result/>).

The modeled 3D structure was submitted to the ElliPro (<http://tools.iedb.org/elliPro/>) prediction tool to filter out the antigenic residues. The minimum score and maximum

TABLE 2: List of the most promising B-cell epitopes and their surface and antigenicity.

Start	End	Peptide	Length	Surface score (Emini's surface threshold = 1.000)	Antigenicity score (Kolaskar's test = 1.025)
129	134	AYFKEH	6	1.502	1.034
191	199	VDKESLYTK	9	2.48	1.032
190	199	HVDKESLYTK	10	2.648	1.04

TABLE 3: List of the promising discontinuous B-cell epitopes.

No.	Residues	Number of residues	Score
1	T300, G301, I302, R303, D304, Y305, V306, L307, N308, K309, K310, D311, Y312, I313, M314, S315, M316, V317, G318, N319, P320, E321, G322, A323, D324, K325, P326, N327, K328, K329, F330, F331, E339, K342	34	0.867
2	D332, P333, R334, V335, W336	5	0.749
3	V3, Q4, E5, V6, L7, K8, Y25, E28, H29, K30, F31, K55, S56, A156, T157, V159, K160, K163, G177, I178, T179, G180, G181, E182, E183, D184, G185, V186, N187, N188, E189, H190, V191, D192, K193, E194, S195, L196, Y197, T198, K199, P200, E201, F204, A205, E208, A209, A211, P212, I213, S214, P215, A222, F223, G224, Q231, A232, G233, N234, V235, V236, L237, S238, P239, E240, A243, D244, K247, Y248, A249, A250, E251, K252, T253, G254, A255, P256, A257, G258, S259, K260, P261, S272, T273, Q274, E275, N278, T279, N282, N283, T357, K358, N359, T360, L361	95	0.669
4	V15, G16, A71, G72, K73, G74, V75, S76, N77, D78, G79, Q80, N81, A82, I84, R85, C112, A113, K114, L117, P118, D121, G122, L124, E125, A126, E128, A129, Y130, F131, K132, E133, H134, G135, E136, P137, L138, R164, A166, A167, M168, N169, Q170	43	0.668
5	L146, S147, E148, E149, T150, D151, D152, E153	8	0.582
6	R9, K10, T11, G12, I14, R52, D53, A98, P99, A100, Y101, G102, I103	13	0.514

distance (Angstrom) were calibrated in the default mode with a score of 0.5 and 6, respectively [60].

2.4. Prediction of MHC Class I Binding Epitopes. The peptides' binding affinity to MHC I molecules was defined by the IEDB MHC I prediction tool at <http://tools.iedb.org/mhc1>. The binding affinity of fructose bisphosphate aldolase peptides to MHC I molecules was obtained using the artificial neural network (ANN) method. All conserved epitopes that bind to MHC I alleles at score ≤ 500 half-maximal inhibitory concentrations (IC₅₀) with peptides that have a length of 9 amino acids were selected for further analysis [49, 61–66].

2.5. MHC Class II Binding Predictions. Prediction of peptide binding affinity to MHC II molecules was defined by the IEDB MHC II prediction tool at <http://tools.iedb.org/mhcii/result/>. MHC II molecules have the ability to bind peptides with different lengths which make the prediction accuracy debatable. For MHC II binding prediction, human allele reference sets were used. The prediction method was selected as NN-align to assess both the binding affinity and MHC II binding core epitopes with a length of 9 amino acid peptides at score IC₅₀ of 100 [49, 67].

2.6. Population Coverage Calculation. The candidate epitopes of MHC I and MHC II and combined binding of MHC I and MHC II alleles from *Candida glabrata* fructose bisphosphate aldolase protein were employed for population coverage, and the world population was set as a target population for the

selected MHC I and MHC II combined binding alleles using the IEDB population coverage calculation tool at <http://tools.iedb.org/population/> [49, 68].

2.7. Homology Modeling. The reference sequence of *Candida glabrata* fructose bisphosphate aldolase protein was applied to Raptor X for modeling at <http://raptorx.uchicago.edu/>. Then, the 3D structural model of the protein was visualized by using the Chimera tool powered by UCSF [69–73].

2.8. Physicochemical Parameters. The function of vaccines is to enhance the immunogenic response once introduced to the immune system. Thus, it is essential to recognize the physicochemical parameters of the protein using the protein program and BioEdit [54] (available at <https://web.expasy.org/protparam/> and <https://web.expasy.org/protscale/>) [74].

2.9. Molecular Docking Analysis. Molecular docking was performed using Moe 2007. The 3D structures of the promiscuous epitopes were predicted by PEP-FOLD. The crystal structures of HLA-A*02:06 (PDB ID 3OXR) and HLA-DRB1*01:01 (PDB ID 5JLZ) were chosen as a model for molecular docking and were downloaded in a PDB format from the RCSB PDB resource. However, the selected crystal structures were in a complex form with ligands. Thus, to simplify the complex structure of all water molecules, hetero groups and ligands were removed by Discovery Studio Visualizer 2.5. Partial charge and energy minimization were applied for ligands and targets. In terms of the identification

TABLE 4: Promising T-cell epitopes (class MHC I alleles) with their position and IC50 value.

Core epitope	Start	End	Allele	IC50
KYFKRMAAM	160	168	HLA-A*24:02	451.84
	160	168	HLA-A*30:01	232.12
	160	168	HLA-A*31:01	131.22
	160	168	HLA-B*14:02	427.02
	160	168	HLA-C*07:02	149.13
	160	168	HLA-C*12:03	240.46
	160	168	HLA-C*14:02	6.27
	205	213	HLA-A*02:01	154.37
AVHEALAPI	205	213	HLA-A*02:06	9.78
	205	213	HLA-A*30:01	20.96
	205	213	HLA-A*32:01	122.32
	205	213	HLA-A*68:02	55.22
RMAAMNQWL	164	172	HLA-A*02:01	52.44
	164	172	HLA-A*02:06	237.09
	164	172	HLA-A*32:01	79.39
	164	172	HLA-B*15:01	258
	164	172	HLA-C*14:02	482
	61	69	HLA-A*01:01	54.18
QTSNGGAAY	61	69	HLA-A*26:01	89.37
	61	69	HLA-A*29:02	56.68
	61	69	HLA-A*30:02	47.89
	61	69	HLA-B*15:01	111.57
	61	69	HLA-B*15:02	82.52
	61	69	HLA-B*35:01	99.45
YFKEHGEPL	130	138	HLA-B*08:01	295.97
	130	138	HLA-C*03:03	42.03
	130	138	HLA-C*07:02	319.29
	130	138	HLA-C*12:03	26.8
	130	138	HLA-C*14:02	18.47

of the binding groove, the potential binding sites in the crystal structure were recognized using the Alpha Site Finder. Finally, ten independent docking runs were carried out for each peptide. The results were retrieved as binding energies. Best poses for each epitope that displayed the lowest binding energies were visualized using UCSF Chimera 1.13.1 software [72, 75–78].

3. Result

3.1. B-Cell Epitope Prediction. The reference sequence of fructose bisphosphate aldolase from *C. glabrata* was analyzed using a Bepipred linear epitope prediction test; the average binder's score of the protein to B-cell was 0.199 and minimum was -0.009 and 2.424 for a maximum score; all values equal or greater than the default threshold 0.350 which were potentially linear epitopes are shown in Figure 2.

3.1.1. Prediction of Surface Accessibility. In Emini's surface accessibility prediction test, for a potent B-cell epitope, the average surface accessibility area of the Fba1 protein was

scored as 1.000, with a maximum of 7.725 and a minimum of 0.113; all values equal or greater than the default threshold 1.000 were potentially in the surface shown in Figure 3.

3.1.2. Prediction of Epitope Antigenicity. For the Kolaskar and Tongaonkar antigenicity prediction test, the average of antigenicity was 1.025, with a maximum of 1.223 and a minimum of 0.853; all values equal to or greater than the default threshold 1.025 are potential antigenic determinants (see Figure 4). The results of all proposed conserved predicted B-cell epitopes are shown in Table 1. The list of the most promising B-cell epitopes with their surface scores and antigenicity is shown in Table 2.

3.1.3. Discontinuous B-Cell Epitope Prediction. The modeled 3D structure of the Fba1 protein was submitted to the ElliPro prediction tool to filter out the antigenic residues. The minimum score and maximum distance (Angstrom) were calibrated in the default mode with a score of 0.5 and 6, respectively (see Table 3 for more illustrations).

3.2. T-Cell Peptide Prediction

3.2.1. Prediction of MHC I Binding Profile for T Cytotoxic Cell Conserved Epitopes. 114 epitopes were anticipated to interact with different MHC I alleles. The core epitopes KYFKRMAAM and QTSNGGAAY were noticed to be the dominant binders with 7 alleles for each (HLA-A*24:02, HLA-A*30:01, HLA-A*31:01, HLA-B*14:02, HLA-C*07:02, HLA-C*12:03, and HLA-C*14:02) (HLA-A*01:01, HLA-A*26:01, HLA-A*29:02, HLA-A*30:02, HLA-B*15:01, HLA-B*15:02, and HLA-B*35:01) followed by AVHEALAPI, RMAAMNQWL, and YFKEHGEPL which bind with five alleles; these findings are shown in Table 4.

3.2.2. Prediction of MHC II Binding Profile for T Helper Cell Conserved Epitopes. 102 conserved predicted epitopes were found to interact with MHC II alleles. The core epitope LFSSHMLDL is thought to be the top binder as it interacts with 9 alleles (HLA-DRB1*07:01, HLA-DPA1*01, HLA-DPB1*04:01, HLA-DPA1*01:03, HLA-DPB1*02:01, HLA-DPA1*02:01, HLA-DPB1*01:01, HLA-DPA1*03:01, and HLA-DPB1*04:02), followed by IRGSIAAAH which binds to five alleles and VVAALEAAR which also binds with five alleles but with low frequency. Followed by YQAGNVVLS and IAPAYGIPV, these findings are shown in Table 5.

3.3. Population Coverage. The most interesting findings in this test is the population coverage analysis result for the most common binders to MHC I and MHC II alleles each and combined among the world, exhibiting an exceptional coverage with percentages 92.54%, 99.58%, and 98.5%, respectively.

3.3.1. Population Coverage for Isolated MHC I. Five epitopes are given to interact with the most frequent MHC class I alleles: AVHEALAPI, KYFKRMAAM, QTSNGGAAY, RMAAMNQWL, and YFKEHGEPL, representing a considerable coverage against the whole world population. The maximum population coverage percentage over these epitopes is 92.54% (see Figure 5).

TABLE 5: Promising T-cell epitope (class MHC II alleles) with their position and peptide sequence and IC50 value and rank.

Core sequence	Allele	Start	End	Peptide sequence	IC50	Rank
LFSSHMLDL	HLA-DRB1*07:01	132	146	KEHGEPLFSSHMLDL	17.8	3.37
	HLA-DPA1*01	135	149	GEPLFSSHMLDLSEE	93.6	5.05
	HLA-DPB1*04:01	135	149	GEPLFSSHMLDLSEE	93.6	5.05
	HLA-DPA1*01:03	133	147	EHGEPLFSSHMLDLS	46	4.82
	HLA-DPB1*02:01	133	147	EHGEPLFSSHMLDLS	46	4.82
	HLA-DPA1*02:01	134	148	HGEPLFSSHMLDLSE	59	6.3
	HLA-DPB1*01:01	134	148	HGEPLFSSHMLDLSE	59	6.3
	HLA-DPA1*03:01	135	149	GEPLFSSHMLDLSEE	12	1.14
	HLA-DPB1*04:02	135	149	GEPLFSSHMLDLSEE	12	1.14
IRGSIAAAH	HLA-DRB1*01:01	81	95	NASIRGSIAAAHYIR	31.5	15.98
	HLA-DRB1*04:01	81	95	NASIRGSIAAAHYIR	86.5	7.02
	HLA-DRB5*01:01	81	95	NASIRGSIAAAHYIR	7.3	1.55
	HLA-DQA1*01:02	80	94	QNASIRGSIAAAHYI	59.3	3.74
	HLA-DQB1*06:02	80	94	QNASIRGSIAAAHYI	59.3	3.74
	HLA-DQA1*05:01	81	95	NASIRGSIAAAHYIR	4.6	0.27
	HLA-DQB1*03:01	81	95	NASIRGSIAAAHYIR	4.6	0.27
YQAGNVVLS	HLA-DRB1*01:01	227	241	HGVYQAGNVVLSPEI	19.7	11.15
	HLA-DRB1*09:01	227	241	HGVYQAGNVVLSPEI	80.9	5.58
	HLA-DQA1*01:02	227	241	HGVYQAGNVVLSPEI	91.3	6.42
	HLA-DQB1*06:02	227	241	HGVYQAGNVVLSPEI	91.3	6.42
	HLA-DQA1*05:01	224	238	GNVHGVYQAGNVVLS	7.9	0.96
	HLA-DQB1*03:01	224	238	GNVHGVYQAGNVVLS	7.9	0.96
VVAALEAAR	HLA-DRB1*03:01	41	55	SSTVVAALEAARDAK	50.9	2.91
	HLA-DRB1*09:01	41	55	SSTVVAALEAARDAK	95.1	6.59
	HLA-DRB5*01:01	41	55	SSTVVAALEAARDAK	15	3.71
	HLA-DQA1*01:02	40	54	SSSTVVAALEAARDA	38.1	1.93
	HLA-DQB1*06:02	40	54	SSSTVVAALEAARDA	38.1	1.93
	HLA-DQA1*05:01	42	56	STVVAALEAARDAKS	16.2	2.87
IAPAYGIPV	HLA-DQB1*03:01	42	56	STVVAALEAARDAKS	16.2	2.87
	HLA-DRB1*01:01	94	108	IRSIAPAYGIPVVLH	12.1	6.74
	HLA-DRB1*07:01	91	105	AHYIRSIAPAYGIPV	34.1	6.37
	HLA-DRB1*15:01	94	108	IRSIAPAYGIPVVLH	79.2	8.07
	HLA-DQA1*05:01	94	108	IRSIAPAYGIPVVLH	16.5	2.94
	HLA-DQB1*03:01	94	108	IRSIAPAYGIPVVLH	16.5	2.94

3.3.2. *Population Coverage for Isolated MHC II.* Three epitopes were assumed to interact with the most frequent MHC class II alleles (IRGSIAAAH, LFSSHMLDL, and VVAALEAAR) with a percentage of 99.58%. The LFSSHMLDL epitope shows an exceptional result for the population coverage test for MHC II binding affinity of 96.60% globally (see Figure 6).

3.3.3. *Population Coverage for MHC I and MHC II Alleles Combined.* Regarding the combined MHC I and MHC II alleles, five epitopes were supposed to interact with the most predominant MHC class I and MHC class II alleles (IAPAYGIPV, AAFGNVHGV, VVAALEAAR, YIRSTIAPAY, and YQAGMVVLS), representing a significant global coverage by the IEDB population coverage tool which revealed coverage with percentage of 98.50% as shown in Figure 7.

3.4. *Homology Modeling.* The 3-dimensional structure of the fructose bisphosphate aldolase protein from *C. glabrata* and the most promising peptides binding to MHC class II by using the Chimera tool powered by UCSF are shown in Figure 8.

3.5. *Physicochemical Parameters.* The length of fructose bisphosphate aldolase protein is 361 amino acids, and its molecular weight is 39356.3. Theoretical pI is 5.49 which explain the pH of the protein. Total numbers of negatively and positively charged residues that contain the fructose bisphosphate aldolase protein are (Asp+Glu): 47 and (Arg+Lys): 35, respectively. Also, the number of atoms that compose this protein is 5488 which presented as flowing: carbon 1752, hydrogen 2716, nitrogen 470, oxygen 538, and sulfur

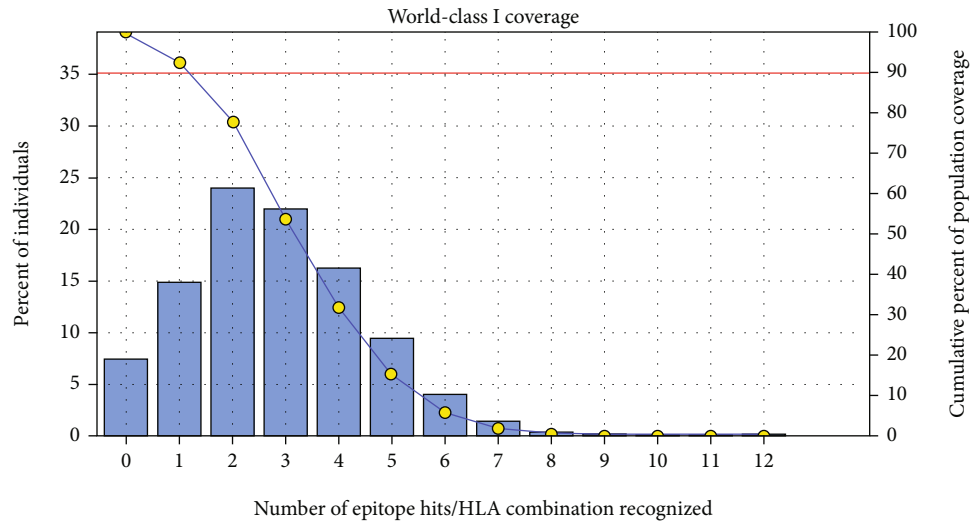


FIGURE 5: Global coverage for the top five MHC I peptides (AVHEALAPI, KYFKRMAAM, QTSNGGAAAY, RMAAMNQWL, and YFKEHGEPL). Note: in the graph, the line (-o-) represents the cumulative percentage of population coverage of the epitopes; the bars represent the population coverage for each epitope.

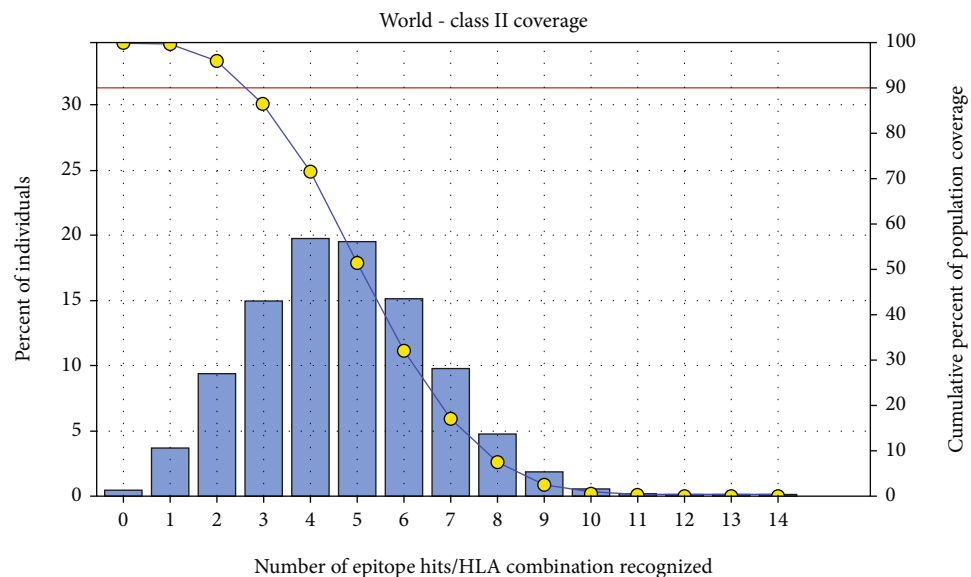


FIGURE 6: Global proportion for the top five MHC II IRGSIAAAH, LFSSHMLDL, and VVAALEAAR. Notes: in the graph, the line (-o-) represents the cumulative percentage of population coverage of the epitopes; the bars represent the population coverage for each epitope.

12. N-terminal of the sequence considered is M (Met). The half-life of the fructose biphosphate aldolase protein estimate is 30 hours (mammalian reticulocytes, in vitro) and more than 20 hours (yeast, in vivo). The aliphatic index and the grand average of hydropathicity (GRAVY) value of vaccine were determined as 80.55 and -0.264 , respectively. Instability of the fructose biphosphate aldolase protein is computed to be 29.93, meaning the protein is stable [74]. The amino acids that compose the protein fructose biphosphate aldolase with their molecular weights are shown in Table 6 and Figure 9.

3.6. *Molecular Docking*. The best epitopes that displayed the lowest binding energies visualized by using UCSF chimera 1.13.1 software are shown in Table 7 and Figures 10–25.

4. Discussion

In the present study, we predicted the most conserved and immunogenic B- and T-cell epitopes from Fba1 protein of *C. Glabrata* by using the immunoinformatics approach in order to develop an effective epitope-based vaccine against this fungal pathogen which has emerged in recent years as a

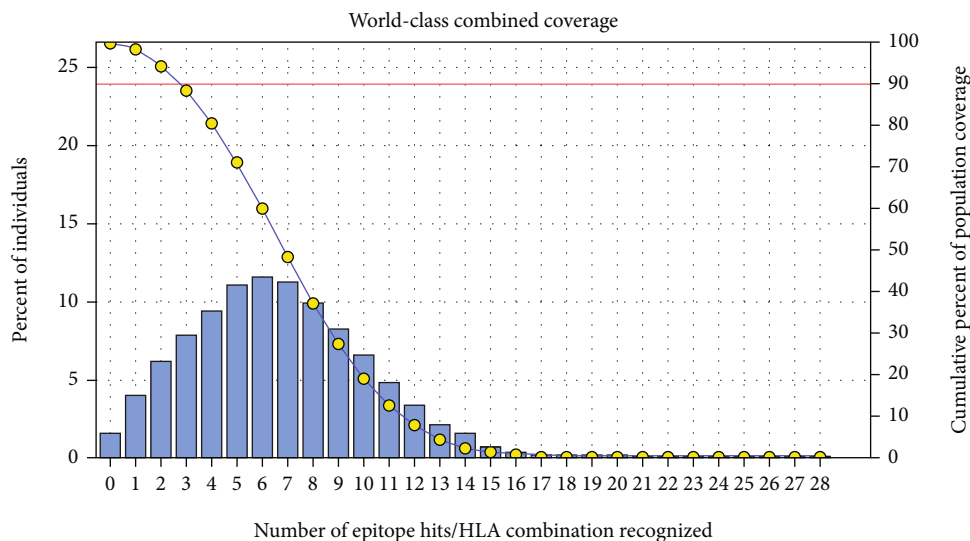


FIGURE 7: Global population proportion for the top five MHC I and II epitopes in combined mode (IAPAYGIPV, AAFGNVHGV, VVAALEAAR, YIRSTIAPAY, and YQAGMVVLS). Notes: in the graphs, the line (-o-) represents the cumulative percentage of population coverage of the epitopes; the bars represent the population coverage for each epitope.

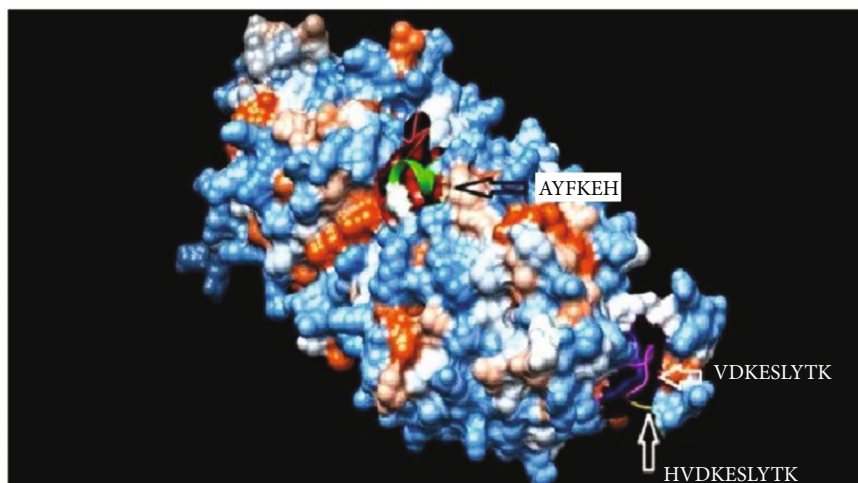


FIGURE 8: Structural position of the promising B-cell epitope (AYFKEH (in purple color), VDKESELYTK (in yellow color), and HVDKESELYTK (in red color)) in 3-dimensional structure of the fructose biphosphate aldolase protein from *C. glabrata* using Chimera tool powered by UCSF.

serious health problem especially among immunosuppressed and hospitalized patients [7]. A previous study conducted by de Klerk et al. [79] showed that the Fba1 protein has the ability to provoke immune responses in human against *M. mycetomatis* [79]. Also, several recent publications have used the Fba1 protein as a strong antigenic target for predicting B- and T-cell epitopes in order to design promising vaccines against fungal and bacterial pathogens such as *M. mycetomatis*, *P. aeruginosa*, *L. monocytogenes*, and *S. mansoni* by using in silico tools [80–83]. Hence, there are more studies to explore the fructose biphosphate aldolase protein immunogenic role and the possibility to find common conserved epitopes for different organisms.

The principle of using a cocktail of B- and T-cell epitopes in the epitope-based vaccine to trigger humoral as well as cellular mediated immune response is very promising to clear infection instead of humoral or cellular immunity alone, and it was applied before to enhance protection against different kinds of infectious diseases [84, 85]. In this study, the analysis of the Fba1 protein revealed 11 effective epitopes for B-cells (AYFKEH, VDKESELYTK, and HVDKESELYTK) and T-cells (AVHEALAPI, KYFKRMAAM, QTSNGGAAY, RMAAMNQWL, YFKEH-GEPL, IRGSIAAAH, LFSSHMLDL, and VVAALEAAR).

However, the molecular docking, which evaluates the binding affinity to MHC molecules [51, 52], showed that the peptides QTSNGGAAY and LFSSHMLDL are the best

TABLE 6: Amino acid composition of the protein (fructose biphosphate aldolase) with their number and molecular weight (Mol%) using BioEdit software version 7.0.5.3.

Amino acid	Number	Mol%	Amino acid	Number	Mol%
Ala A	39	10.80	Leu L	23	6.37
Cys C	3	0.83	Met M	9	2.49
Asp D	21	5.82	Asn N	19	5.26
Glu E	26	7.20	Pro P	15	4.16
Phe F	14	3.88	Gln Q	8	2.22
Gly G	30	8.31	Arg R	10	2.77
His H	12	3.32	Ser S	23	6.37
Ile I	20	5.54	Thr T	17	4.71
Lys K	25	6.93	Val V	29	8.03
Trp W	3	0.83	Tyr Y	15	4.16

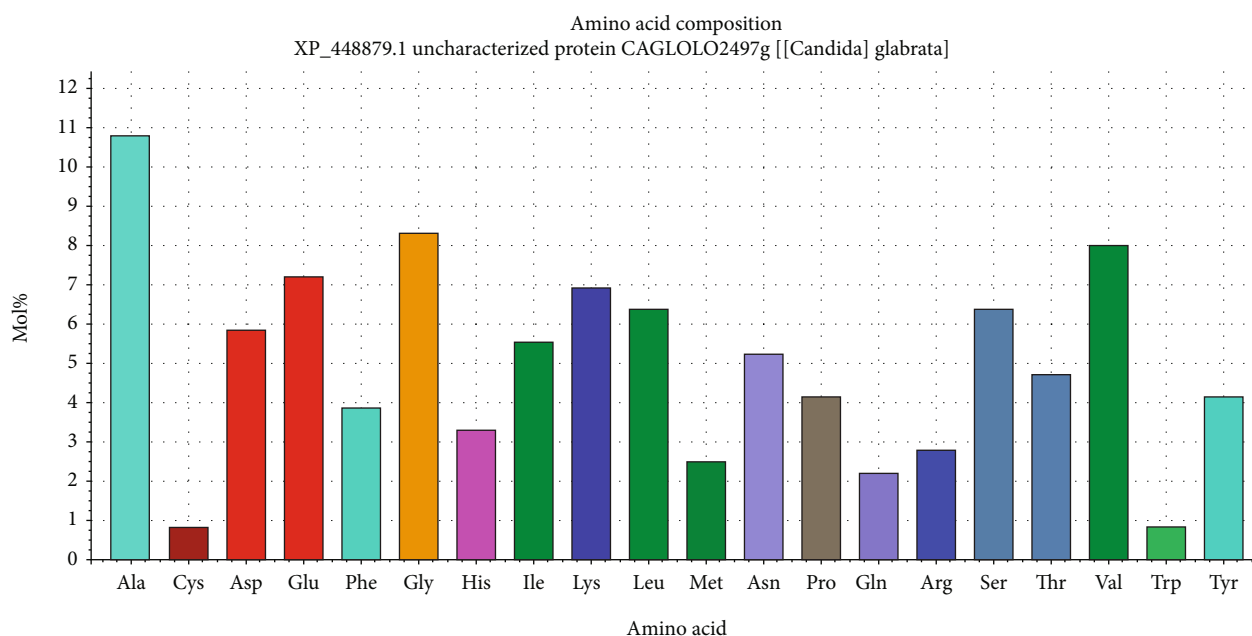


FIGURE 9: Graph showing amino acid composition of fructose biphosphate aldolase protein and their molecular weights using BioEdit software 7.0.5.3.

TABLE 7: Docking results of the most promiscuous epitopes that show the best binding affinity.

Epitope	Binding MHC molecule	Binding energy (ΔG^* kcal/mol)
AVHEALAPI	HLA-A*02:06	-15.8010
KYFKRMAAM	HLA-A*02:06	-20.5935
QTSNGGAAY	HLA-A*02:06	-30.5467
RMAAMNQWL	HLA-A*02:06	-20.6392
YFKEHGEPL	HLA-A*02:06	-16.7505
IRGSIAAAH	HLA-DRB1*01:01	-20.6557
LFSSHMLDL	HLA-DRB1*01:01	-25.5732
VVAALEAAR	HLA-DRB1*01:01	-19.8404

*Global energy: it is the energy required to estimate the strength of association between the epitope within the active.

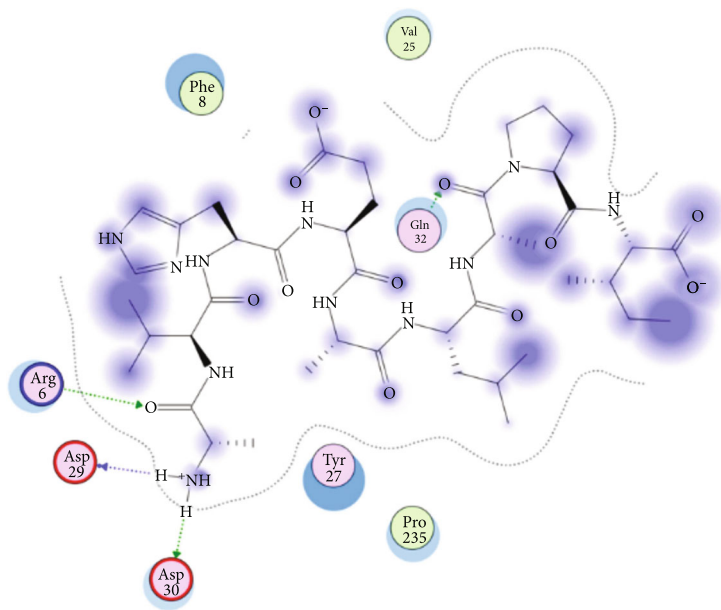


FIGURE 10: Illustration of the 2D interaction of the best docking poses of AVHEALAPI in the binding sites of HLA-A*02:06.

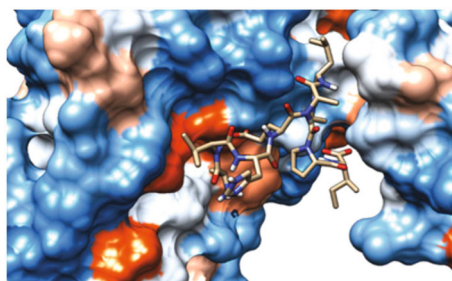


FIGURE 11: Illustration of the 3D interaction of the best docking poses of AVHEALAPI in the binding sites of HLA-A*02:06.

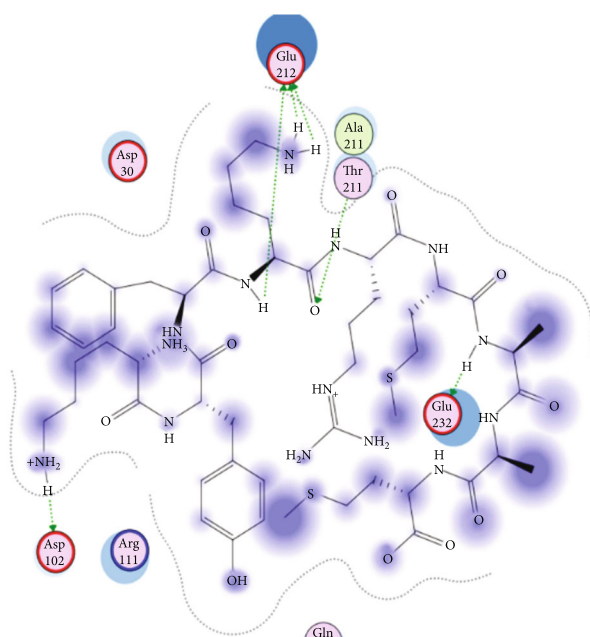


FIGURE 12: Illustration of the 3D interaction of the best docking poses of KYFKRMAAM in the binding sites of HLA-A*02:06.

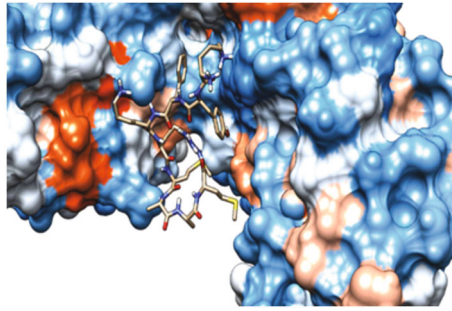


FIGURE 13: Illustration of the 3D interaction of the best docking poses of KYFKRMAAM in the binding sites of HLA-A*02:06.

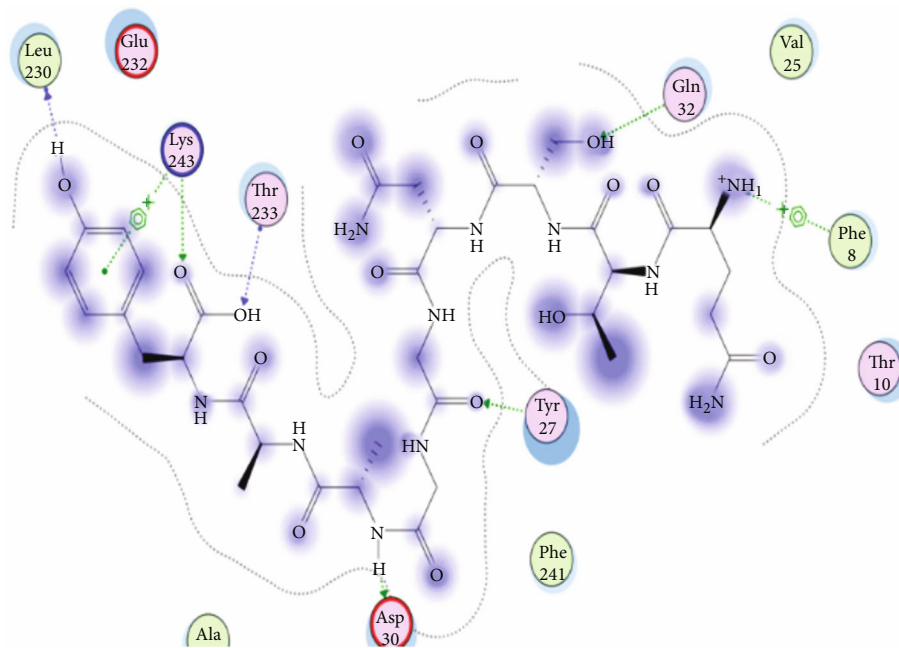


FIGURE 14: Illustration of the 2D interaction of the best docking poses of QTSNGGAAY in the binding sites of HLA-A*02:06.

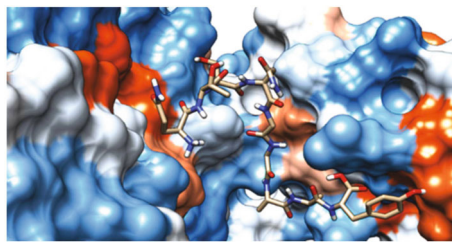


FIGURE 15: Illustrate the 2D interaction of the best docking poses of QTSNGGAAY in the binding sites of HLA-A*02:06.

candidates for designing an effective epitope-based vaccine against *C. glabrata*.

After retrieving the various sequences of *C. glabrata* fructose biphosphate aldolase protein, the protein reference sequence was submitted to the Bepipred linear epitope prediction test, Emini surface accessibility test, and Kolaskar

and Tongaonkar antigenicity test in the IEDB, to determine the affinity of B-cell epitopes and their position regarding the surface and their immunogenicity. Three peptides have passed (AYFKEH, VDKEPLYTK, and HVDKEPLYTK) in all the prediction tests shown in Tables 1 and 2 and Figures 2–4. However, the MHC I binding prediction tool

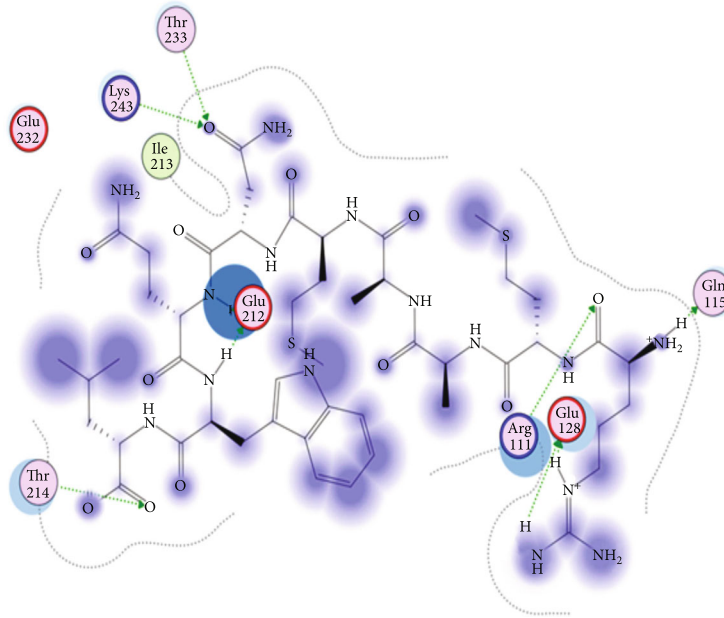


FIGURE 16: Illustration of the 2D interaction of the best docking poses of RMAAMNQWL in the binding sites of HLA-A*02:06.

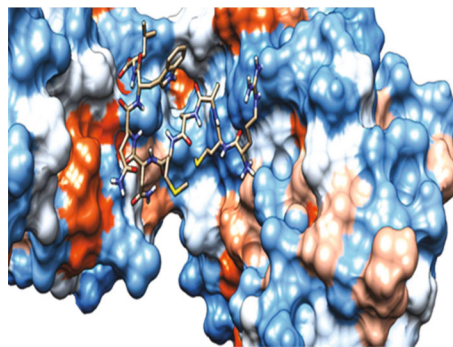


FIGURE 17: Illustration of the 2D interaction of the best docking poses of RMAAMNQWL in the binding sites of HLA-A*02:06.

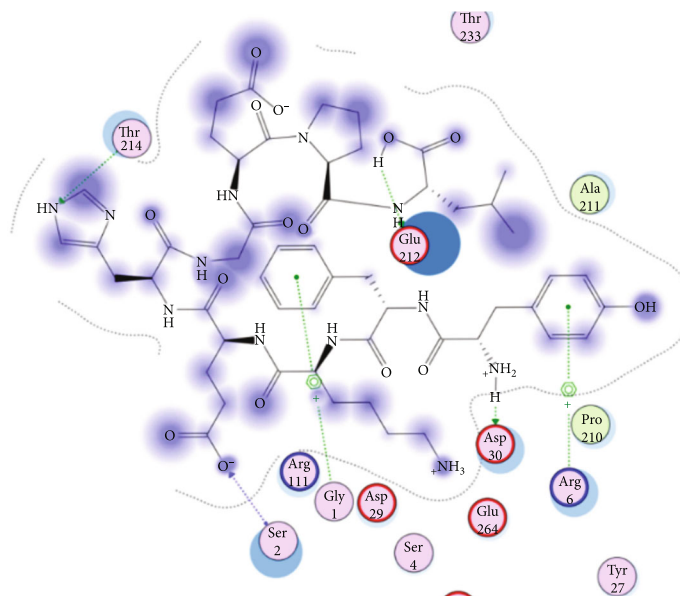


FIGURE 18: Illustration of the 3D interaction of the best docking poses of YFKEHGEPL in the binding sites of HLA-A*02:06.

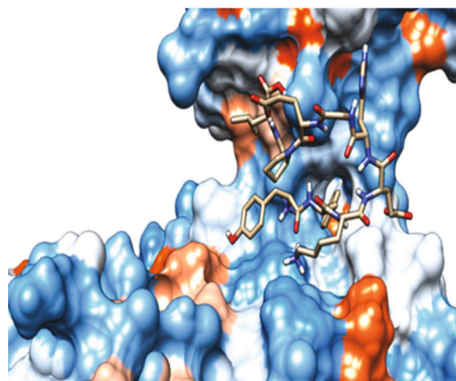


FIGURE 19: Illustration of the 3D interaction of the best docking poses of YFKEHGEP in the binding sites of HLA-A*02:06.

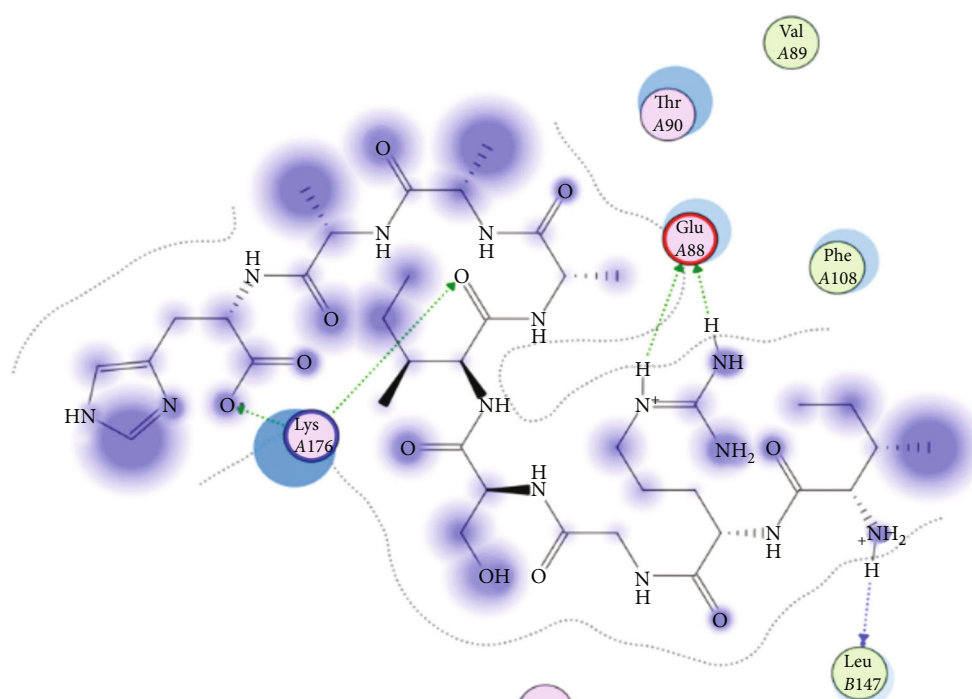


FIGURE 20: Illustration of the 3D interaction of the best docking poses of IRGSIAAAH in the binding sites of HLA-DRB1*01:01.

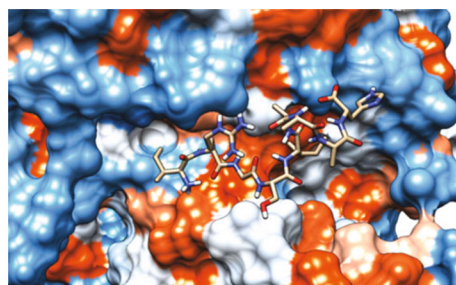


FIGURE 21: Illustration of the 3D interaction of the best docking poses of IRGSIAAAH in the binding sites of HLA-DRB1*01:01.

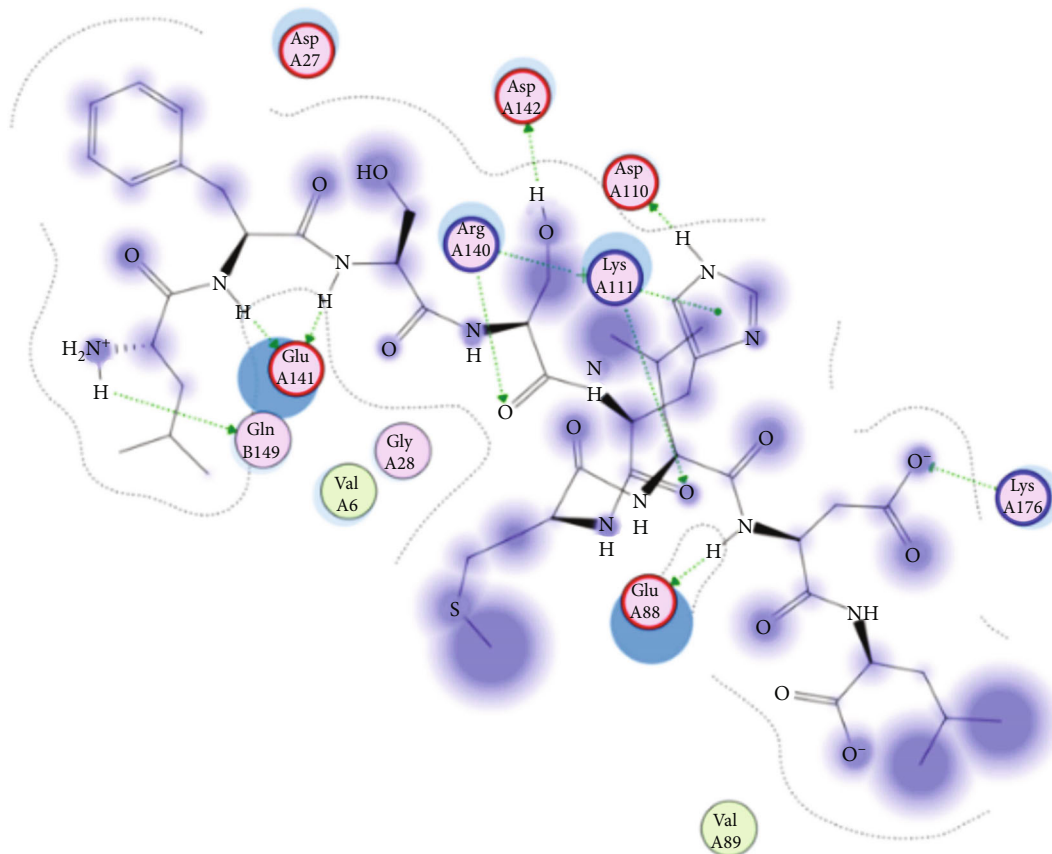


FIGURE 22: Illustration of the 3D interaction of the best docking poses of LFSSHMLDL in the binding sites of HLA-DRB1*01:01.

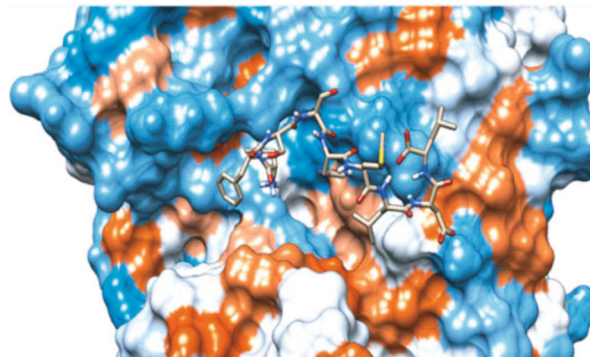


FIGURE 23: Illustration of the 3D interaction of the best docking poses of LFSSHMLDL in the binding sites of HLA-DRB1*01:01.

using an artificial neural network (ANN) [61] with half maximal inhibitory concentration (IC_{50}) ≤ 500 revealed 114 conserved peptides interacting with various MHC I alleles. Three peptides were noticed to have the highest affinity in corresponding to their interaction with MHC I alleles. The peptide YIRSIAPAY from 93 to 101 had the affinity with 8 alleles to interact with HLA-A*26:01, HLA-A*29:02, HLA-B*15:01, HLA-A*30:02, HLA-B*15:02, HLA-B*35:01, HLA-C*14:02, and HLA-C*12:03, followed in order by KYFKRMAAM from 160 to 168 which interacts with 7 alleles

(HLA-A*24:02, HLA-A*31:01, HLA-A*30:01, HLA-B*14:02, HLA-C*07:02, HLA-C*14:02, and HLA-C*12:03) and QTSNGGAAY from 61 to 69 which interacts with 7 alleles (HLA-A*01:01, HLA-A*26:01, HLA-A*30:02, HLA-A*29:02, HLA-B*15:02, HLA-B*15:01, and HLA-B*35:01) (see Table 4), while MHC II binding prediction tool using NN-align [67] with half-maximal inhibitory concentration (IC_{50}) ≤ 100 revealed 102 conserved peptides that interact with various MHC II alleles. Two peptides (LFSSHMLDL and YIRSIAPAY) were noted to have the highest affinity in

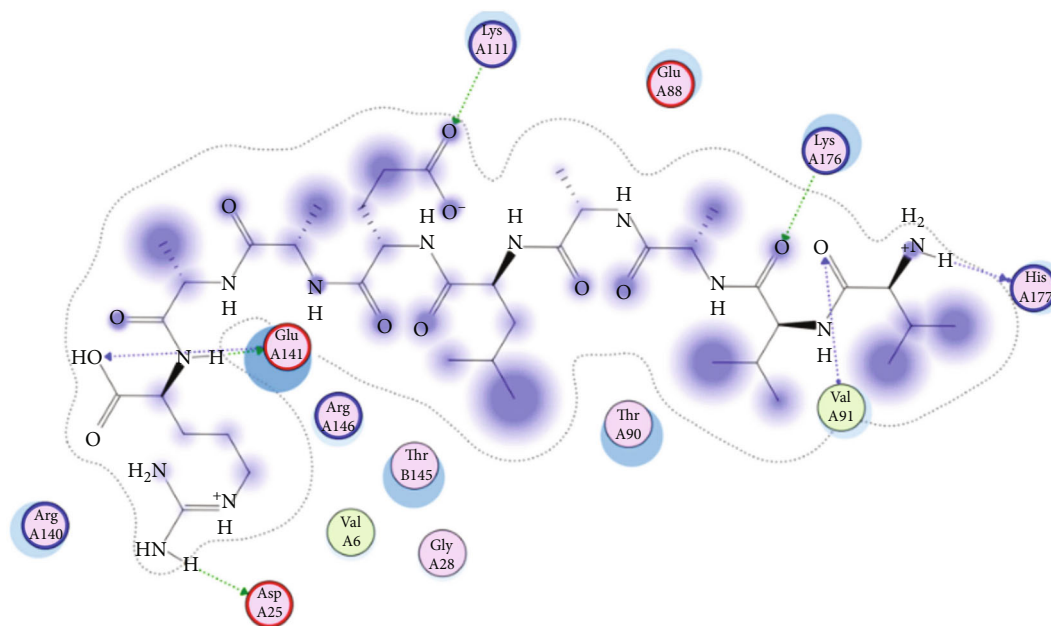


FIGURE 24: Illustration of the 2D interaction of the best docking poses of VVAALEAAR in the binding sites of HLA-DRB1*01:01.

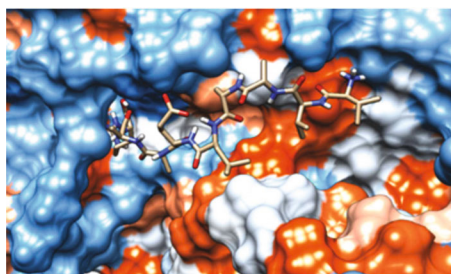


FIGURE 25: Illustration of the 2D interaction of the best docking poses of VVAALEAAR in the binding sites of HLA-DRB1*01:01.

corresponding to their interaction with MHC II alleles; both had the affinity to interact with 9 MHC II alleles (see Table 5). Moreover, the predicted epitopes which have the high affinity to interact with MHC I, MHC II, and combined MHC I with MHC II international alleles were analyzed by population coverage resource in the IEDB [68]. The population coverage of the five most promising epitopes (AVHEALAPI, KYFKRMAAM, QTSNGGAAY, RMAAMNQWL, and YFKEHGEPL) for MHC I alleles was 92.54%, while for the three epitopes (IRGSIAAAH, LFSSHMLDL, and VVAALEAAR) that showed high affinity to MHC II alleles, it was 99.58% throughout the world according to the IEDB database as shown in Figures 5 and 6. It should be noted that the population coverage of the five most promising epitopes that exhibited binding affinity to both MHC I and MHC II alleles (IAPAYGIPV, AAFGNVHGV, VVAALEAAR, YIRSTIAPAY, and YQAGMVVLS) was 98.50% globally (see Figure 7). However, the molecular docking revealed that the epitopes QTSNGGAAY and LFSSHMLDL have high binding energy to MHC molecules HLA-A*02:06 and HLA-DRB1*01:01, respectively, which indicate favored affinity and stability in the epitope-molecule complex shown

in Table 7 and Figures 10–25. This study was limited by being strictly computational, and more in vitro and in vivo studies to prove the effectiveness of the proposed peptides are highly recommended.

5. In Conclusion

The epitope-based vaccines predicted by using immunoinformatics tools have remarkable advantages over the conventional vaccines in that they are more specific, less time consuming, safe, less allergic, and more antigenic. Further in vivo and in vitro experiments are needed to prove the effectiveness of the best candidate's epitopes QTSNGGAAY and LFSSHMLDL. To the best of our knowledge, this is the first study that has predicted B- and T-cell epitopes from the Fba1 protein by using in silico tools in order to design an effective epitope-based vaccine against *C. glabrata*.

Data Availability

The data used to support the findings of this study are available from the corresponding author upon request.

Conflicts of Interest

The authors declare that there are no conflicts of interest.

Acknowledgments

The authors are grateful to Africa City of Technology, Khartoum, Sudan.

References

- [1] D. Bitar, O. Lortholary, Y. le Strat et al., "Population-based analysis of invasive fungal infections, France, 2001-2010," *Emerging Infectious Diseases*, vol. 20, no. 7, pp. 1149–1155, 2014.
- [2] A. A. Cleveland, M. M. Farley, L. H. Harrison et al., "Changes in incidence and antifungal drug resistance in candidemia: results from population-based laboratory surveillance in Atlanta and Baltimore, 2008-2011," *Clinical Infectious Diseases*, vol. 55, no. 10, pp. 1352–1361, 2012.
- [3] B. J. Kullberg and M. C. Arendrup, "Invasive candidiasis," *The New England Journal of Medicine*, vol. 373, no. 15, pp. 1445–1456, 2015.
- [4] S. S. Magill, J. R. Edwards, W. Bamberg et al., "Multistate point-prevalence survey of health care-associated infections," *The New England Journal of Medicine*, vol. 370, no. 13, pp. 1198–1208, 2014.
- [5] B. Gonçalves, C. Ferreira, C. T. Alves, M. Henriques, J. Azeredo, and S. Silva, "Vulvovaginal candidiasis: epidemiology, microbiology and risk factors," *Critical Reviews in Microbiology*, vol. 42, no. 6, pp. 905–927, 2016.
- [6] J. Perlroth, B. Choi, and B. Spellberg, "Nosocomial fungal infections: epidemiology, diagnosis, and treatment," *Medical Mycology*, vol. 45, no. 4, pp. 321–346, 2007.
- [7] M. A. Pfaller and D. J. Diekema, "Epidemiology of invasive candidiasis: a persistent public health problem," *Clinical Microbiology Reviews*, vol. 20, no. 1, pp. 133–163, 2007.
- [8] N. Yapar, "Epidemiology and risk factors for invasive candidiasis," *Therapeutics and Clinical Risk Management*, vol. 10, pp. 95–105, 2014.
- [9] S. Silva, M. Negri, M. Henriques, R. Oliveira, D. W. Williams, and J. Azeredo, "Candida glabrata, Candida parapsilosis and Candida tropicalis: biology, epidemiology, pathogenicity and antifungal resistance," *FEMS Microbiology Reviews*, vol. 36, no. 2, pp. 288–305, 2012.
- [10] M. E. Brandt, "Candida and candidiasis," *Emerging Infectious Diseases*, vol. 8, no. 8, pp. 876–876, 2002.
- [11] G. P. Wormser and K. J. Ryan, "Medically important fungi: a guide to identification, 4th edition Davise H. Larone Washington, D.C.: American Society for Microbiology Press, 2002. 409 pp., illustrated. \$79.95 (cloth)," *Clinical Infectious Diseases*, vol. 37, no. 9, pp. 1281–1281, 2003.
- [12] L. Kasper, K. Seider, and B. Hube, "Intracellular survival of Candida glabrata in macrophages: immune evasion and persistence," *FEMS Yeast Research*, vol. 15, no. 5, p. fov042, 2015.
- [13] R. Atanasova, A. Angoulvant, M. Tefit et al., "A mouse model for Candida glabrata hematogenous disseminated infection starting from the gut: evaluation of strains with different adhesion properties," *PLoS One*, vol. 8, no. 7, article e69664, 2013.
- [14] B. Dujon, D. Sherman, G. Fischer et al., "Genome evolution in yeasts," *Nature*, vol. 430, no. 6995, pp. 35–44, 2004.
- [15] K. M. Ahmad, J. Kokošar, X. Guo, Z. Gu, O. P. Ishchuk, and J. Piškur, "Genome structure and dynamics of the yeast pathogen Candida glabrata," *FEMS Yeast Research*, vol. 14, no. 4, pp. 529–535, 2014.
- [16] E. López-Fuentes, G. Gutiérrez-Escobedo, B. Timmermans, P. Van Dijck, A. D. L. Peñas, and I. Castaño, "Candida glabrata's genome plasticity confers a unique pattern of expressed cell wall proteins," *Journal of Fungi*, vol. 4, no. 2, p. 67, 2018.
- [17] T. Gabaldón, T. Martin, M. Marcet-Houben et al., "Comparative genomics of emerging pathogens in the Candida glabrata clade," *BMC Genomics*, vol. 14, no. 1, p. 623, 2013.
- [18] P. W. J. de Groot, E. A. Kraneveld, Q. Y. Yin et al., "The cell wall of the human pathogen Candida glabrata: differential incorporation of novel adhesin-like wall proteins," *Eukaryotic Cell*, vol. 7, no. 11, pp. 1951–1964, 2008.
- [19] B. Timmermans, A. D. L. Peñas, I. Castaño, and P. Van Dijck, "Adhesins in Candida glabrata," *Journal of Fungi*, vol. 4, no. 2, p. 60, 2018.
- [20] NCBI, *Protein Database* <https://www.ncbi.nlm.nih.gov/protein>.
- [21] A. Nunez-Beltran, E. Lopez-Romero, and M. Cuellar-Cruz, "Identification of proteins involved in the adhesion of Candida species to different medical devices," *Microbial Pathogenesis*, vol. 107, pp. 293–303, 2017.
- [22] V. Cabezón, V. Vialás, A. Gil-Bona et al., "Apoptosis of Candida albicans during the interaction with murine macrophages: proteomics and cell-death marker monitoring," *Journal of Proteome Research*, vol. 15, no. 5, pp. 1418–1434, 2016.
- [23] M. D. Leach, D. A. Stead, E. Argo, D. M. MacCallum, and A. J. P. Brown, "Molecular and proteomic analyses highlight the importance of ubiquitination for the stress resistance, metabolic adaptation, morphogenetic regulation and virulence of Candida albicans," *Molecular Microbiology*, vol. 79, no. 6, pp. 1574–1593, 2011.
- [24] K. H. Lee, S. Y. Kim, J. H. Jung, and J. Kim, "Proteomic analysis of hyphae-specific proteins that are expressed differentially in cakem1/cakem1 mutant strains of Candida albicans," *Journal of Microbiology*, vol. 48, no. 3, pp. 365–371, 2010.
- [25] M. Martínez-Gomariz, P. Perumal, S. Mekala, C. Nombela, W. L. J. Chaffin, and C. Gil, "Proteomic analysis of cytoplasmic and surface proteins from yeast cells, hyphae, and biofilms of Candida albicans," *Proteomics*, vol. 9, no. 8, pp. 2230–2252, 2009.
- [26] C. L. Medrano-Díaz, A. Vega-González, E. Ruiz-Baca, A. Moreno, and M. Cuéllar-Cruz, "Moonlighting proteins induce protection in a mouse model against Candida species," *Microbial Pathogenesis*, vol. 124, pp. 21–29, 2018.
- [27] C. Compagno, B. M. Ranzi, and E. Martegani, "The promoter of Saccharomyces cerevisiae FBA1 gene contains a single positive upstream regulatory element," *FEBS Letters*, vol. 293, no. 1-2, pp. 97–100, 1991.
- [28] D. A. Fell, "Metabolic control analysis: a survey of its theoretical and experimental development," *The Biochemical Journal*, vol. 286, no. 2, pp. 313–330, 1992.
- [29] J. J. Marsh and H. G. Leberer, "Fructose-bisphosphate aldolases: an evolutionary history," *Trends in Biochemical Sciences*, vol. 17, no. 3, pp. 110–113, 1992.
- [30] H. G. Schwelberger, S. D. Kohlwein, and F. Paltauf, "Molecular cloning, primary structure and disruption of the structural gene of aldolase from Saccharomyces cerevisiae," *European Journal of Biochemistry*, vol. 180, no. 2, pp. 301–308, 1989.

- [31] X. Gao, S. Bao, X. Xing et al., "Fructose-1,6-bisphosphate aldolase of *Mycoplasma bovis* is a plasminogen-binding adhesin," *Microbial Pathogenesis*, vol. 124, pp. 230–237, 2018.
- [32] F. M. Klis, G. J. Sosinska, P. W. J. de Groot, and S. Brul, "Covalently linked cell wall proteins of *Candida albicans* and their role in fitness and virulence," *FEMS Yeast Research*, vol. 9, no. 7, pp. 1013–1028, 2009.
- [33] M. D. Ramirez-Quijas, E. Lopez-Romero, and M. Cuellar-Cruz, "Proteomic analysis of cell wall in four pathogenic species of *Candida* exposed to oxidative stress," *Microbial Pathogenesis*, vol. 87, pp. 1–12, 2015.
- [34] I. Serrano-Fujarte, E. Lopez-Romero, and M. Cuellar-Cruz, "Moonlight-like proteins of the cell wall protect sessile cells of *Candida* from oxidative stress," *Microbial Pathogenesis*, vol. 90, pp. 22–33, 2016.
- [35] A. Y. Jong, S. H. M. Chen, M. F. Stins, K. S. Kim, T. L. Tuan, and S. H. Huang, "Binding of *Candida albicans* enolase to plasmin(ogen) results in enhanced invasion of human brain microvascular endothelial cells," *Journal of Medical Microbiology*, vol. 52, no. 8, pp. 615–622, 2003.
- [36] A. Laín, N. Elguezal, E. Amutio, I. F. de Larrinoa, M. D. Moragues, and J. Pontón, "Use of recombinant antigens for the diagnosis of invasive candidiasis," *Clinical & Developmental Immunology*, vol. 2008, article 721950, pp. 1–7, 2008.
- [37] S. Sandini, R. la Valle, S. Deaglio, F. Malavasi, A. Cassone, and F. de Bernardis, "A highly immunogenic recombinant and truncated protein of the secreted aspartic protease family (rSap2t) of *Candida albicans* as a mucosal anticandidal vaccine," *FEMS Immunology and Medical Microbiology*, vol. 62, no. 2, pp. 215–224, 2011.
- [38] A. Rodaki, T. Young, and A. J. Brown, "Effects of depleting the essential central metabolic enzyme fructose-1,6-bisphosphate aldolase on the growth and viability of *Candida albicans*: implications for antifungal drug target discovery," *Eukaryotic Cell*, vol. 5, no. 8, pp. 1371–1377, 2006.
- [39] S. H. I. R. I. N. E. L. H. A. I. K. GOLDMAN, S. H. A. H. A. R. DOTAN, A. M. I. R. TALIAS et al., "Streptococcus pneumoniae fructose-1,6-bisphosphate aldolase, a protein vaccine candidate, elicits Th1/Th2/Th17-type cytokine responses in mice," *International Journal of Molecular Medicine*, vol. 37, no. 4, pp. 1127–1138, 2016.
- [40] J. Huang, H. Zhu, J. Wang et al., "Fructose-1,6-bisphosphate aldolase is involved in *Mycoplasma bovis* colonization as a fibronectin-binding adhesin," *Research in Veterinary Science*, vol. 124, pp. 70–78, 2019.
- [41] S. Brunke and B. Hube, "Two unlike cousins: *Candida albicans* and *C. glabrata* infection strategies," *Cellular Microbiology*, vol. 15, no. 5, pp. 701–708, 2013.
- [42] K. R. Healey and D. S. Perlin, "Fungal resistance to echinocandins and the MDR phenomenon in *Candida glabrata*," *Journal Fungi*, vol. 4, no. 3, 2018.
- [43] L. S. Wilson, C. M. Reyes, M. Stolpman, J. Speckman, K. Allen, and J. Beney, "The direct cost and incidence of systemic fungal infections," *Value in Health*, vol. 5, no. 1, pp. 26–34, 2002.
- [44] C. Clerckx, D. Wilmes, S. Aydin, J. C. Yombi, E. Goffin, and J. Morelle, "*Candida glabrata* renal abscesses in a peritoneal dialysis patient," *Peritoneal Dialysis International*, vol. 32, no. 1, pp. 114–115, 2012.
- [45] G. A. Eschenauer, P. L. Carver, T. S. Patel et al., "Survival in patients with *Candida glabrata* bloodstream infection is associated with fluconazole dose," *Antimicrobial Agents and Chemotherapy*, vol. 62, no. 6, 2018.
- [46] Z. Zhu, Z. Huang, Z. Li, X. Li, C. du, and Y. Tian, "Multiple brain abscesses caused by infection with *Candida glabrata*: a case report," *Experimental and Therapeutic Medicine*, vol. 15, no. 3, pp. 2374–2380, 2018.
- [47] S. Nami, R. Mohammadi, M. Vakili, K. Khezripour, H. Mirzaei, and H. Morovati, "Fungal vaccines, mechanism of actions and immunology: a comprehensive review," *Bio-medicine & Pharmacotherapy*, vol. 109, pp. 333–344, 2019.
- [48] H. Xin, "Effects of immune suppression in murine models of disseminated *Candida glabrata* and *Candida tropicalis* infection and utility of a synthetic peptide vaccine," *Medical Mycology*, vol. 57, no. 6, 2019.
- [49] IEDB, *Immune Epitope Database* <http://tools.iedb.org>.
- [50] R. Vita, J. A. Overton, J. A. Greenbaum et al., "The immune epitope database (IEDB) 3.0," *Nucleic Acids Research*, vol. 43, no. D1, pp. D405–D412, 2015.
- [51] L. Backert and O. Kohlbacher, "Immunoinformatics and epitope prediction in the age of genomic medicine," *Genome Medicine*, vol. 7, no. 1, p. 119, 2015.
- [52] A. A. Bahrami, Z. Payandeh, S. Khalili, A. Zakeri, and M. Bandehpour, "Immunoinformatics: in silico approaches and computational design of a multi-epitope, immunogenic protein," *International Reviews of Immunology*, vol. 38, no. 6, pp. 307–322, 2019.
- [53] Y. He, R. Rappuoli, A. S. De Groot, and R. T. Chen, "Vaccine informatics," *Journal of Biomedicine & Biotechnology*, vol. 2010, Article ID 765762, 2010.
- [54] T. A. Hall, "BioEdit: a user-friendly biological sequence alignment editor and analysis program for Windows 95/98/NT," in *Nucleic acids symposium series*, Information Retrieval Ltd., c1979-c2000, London, 1999.
- [55] P. Haste Andersen, "Prediction of residues in discontinuous B-cell epitopes using protein 3D structures," *Protein Science*, vol. 15, no. 11, pp. 2558–2567, 2006.
- [56] J. E. Larsen, O. Lund, and M. Nielsen, "Improved method for predicting linear B-cell epitopes," *Immunome Research*, vol. 2, no. 1, 2006.
- [57] J. V. Ponomarenko and P. E. Bourne, "Antibody-protein interactions: benchmark datasets and prediction tools evaluation," *BMC Structural Biology*, vol. 7, no. 1, p. 64, 2007.
- [58] E. A. Emini, J. V. Hughes, D. S. Perlow, and J. Boger, "Induction of hepatitis A virus-neutralizing antibody by a virus-specific synthetic peptide," *Journal of Virology*, vol. 55, no. 3, pp. 836–839, 1985.
- [59] A. S. Kolaskar and P. C. Tongaonkar, "A semi-empirical method for prediction of antigenic determinants on protein antigens," *FEBS Letters*, vol. 276, no. 1–2, pp. 172–174, 1990.
- [60] J. Ponomarenko, H.-H. Bui, W. Li et al., "ElliPro: a new structure-based tool for the prediction of antibody epitopes," *BMC Bioinformatics*, vol. 9, no. 1, p. 514, 2008.
- [61] M. Andreatta and M. Nielsen, "Gapped sequence alignment using artificial neural networks: application to the MHC class I system," *Bioinformatics*, vol. 32, no. 4, pp. 511–517, 2016.
- [62] S. Buus, S. L. Lauemøller, P. Worning et al., "Sensitive quantitative predictions of peptide-MHC binding by a 'Query by Committee' artificial neural network approach," *Tissue Antigens*, vol. 62, no. 5, pp. 378–384, 2003.
- [63] C. Lundegaard, K. Lamberth, M. Harndahl, S. Buus, O. Lund, and M. Nielsen, "NetMHC-3.0: accurate web accessible

- predictions of human, mouse and monkey MHC class I affinities for peptides of length 8-11," *Nucleic Acids Research*, vol. 36, 2008.
- [64] C. Lundegaard, O. Lund, and M. Nielsen, "Accurate approximation method for prediction of class I MHC affinities for peptides of length 8, 10 and 11 using prediction tools trained on 9mers," *Bioinformatics*, vol. 24, no. 11, pp. 1397-1398, 2008.
- [65] C. Lundegaard, M. Nielsen, and O. Lund, "The validity of predicted T-cell epitopes," *Trends in Biotechnology*, vol. 24, no. 12, pp. 537-538, 2006.
- [66] M. Nielsen, C. Lundegaard, P. Worning et al., "Reliable prediction of T-cell epitopes using neural networks with novel sequence representations," *Protein Science*, vol. 12, no. 5, pp. 1007-1017, 2003.
- [67] M. Nielsen and O. Lund, "NN-align. An artificial neural network-based alignment algorithm for MHC class II peptide binding prediction," *BMC Bioinformatics*, vol. 10, no. 1, 2009.
- [68] H. H. Bui, J. Sidney, K. Dinh, S. Southwood, M. J. Newman, and A. Sette, "Predicting population coverage of T-cell epitope-based diagnostics and vaccines," *BMC Bioinformatics*, vol. 7, no. 1, p. 153, 2006.
- [69] J. E. Chen, C. C. Huang, and T. E. Ferrin, "RRDistMaps: a UCSF Chimera tool for viewing and comparing protein distance maps," *Bioinformatics*, vol. 31, no. 9, pp. 1484-1486, 2015.
- [70] S. Hertig, T. D. Goddard, G. T. Johnson, and T. E. Ferrin, "Multidomain Assembler (MDA) generates models of large multidomain proteins," *Biophysical Journal*, vol. 108, no. 9, pp. 2097-2102, 2015.
- [71] M. Källberg, H. Wang, S. Wang et al., "Template-based protein structure modeling using the RaptorX web server," *Nature Protocols*, vol. 7, no. 8, pp. 1511-1522, 2012.
- [72] E. F. Pettersen, T. D. Goddard, C. C. Huang et al., "UCSF Chimera—a visualization system for exploratory research and analysis," *Journal of Computational Chemistry*, vol. 25, no. 13, pp. 1605-1612, 2004.
- [73] Z. Yang, K. Lasker, D. Schneidman-Duhovny et al., "UCSF Chimera, MODELLER, and IMP: an integrated modeling system," *Journal of Structural Biology*, vol. 179, no. 3, pp. 269-278, 2012.
- [74] E. Gasteiger, A. Gattiker, C. Hoogland, I. Ivanyi, R. D. Appel, and A. Bairoch, "ExPASy: the proteomics server for in-depth protein knowledge and analysis," *Nucleic Acids Research*, vol. 31, no. 13, pp. 3784-3788, 2003.
- [75] C. C. G. Inc, *Molecular Operating Environment (MOE)*, 2007, <http://www.chemcomp.com>.
- [76] D. S. BIOVIA, *Discovery Studio Visualizer 2.5 ed*, San Diego, Dassault Systèmes, 2009, <https://www.3dsbiovia.com/>.
- [77] Y. Shen, J. Maupetit, P. Derreumaux, and P. Tufféry, "Improved PEP-FOLD approach for peptide and miniprotein structure prediction," *Journal of Chemical Theory and Computation*, vol. 10, no. 10, pp. 4745-4758, 2014.
- [78] P. Thevenet, Y. Shen, J. Maupetit, F. Guyon, P. Derreumaux, and P. Tuffery, "PEP-FOLD: an updated de novo structure prediction server for both linear and disulfide bonded cyclic peptides," *Nucleic Acids Research*, vol. 40, no. W1, pp. W288-W293, 2012.
- [79] N. de Klerk, C. de Vogel, A. Fahal, A. van Belkum, and W. W. J. van de Sande, "Fructose-bisphosphate aldolase and pyruvate kinase, two novel immunogens in *Madurella mycetomatis*," *Medical Mycology*, vol. 50, no. 2, pp. 143-151, 2012.
- [80] M. Elhag, M. Abubaker, N. M. Ahmad, E. M. Haroon, R. M. Alaagib, and M. A. Hassan, "Immunoinformatics prediction of epitope based peptide vaccine against listeria monocytogenes fructose bisphosphate aldolase protein," *BioRxiv*, p. 649111, 2019.
- [81] M. Elhag, R. M. Alaagib, N. M. Ahmed et al., "Design of epitope-based peptide vaccine against pseudomonas aeruginosa fructose bisphosphate aldolase protein using immunoinformatics," *Journal of Immunology Research*, vol. 2020, pp. 1-11, 2020.
- [82] M. Elhag, R. M. Alaagib, E. M. Haroun, N. M. Ahmed, S. O. Abd Albagi, and M. A. Hassan, "Immunoinformatics prediction of epitope based peptide vaccine against schistosoma mansoni fructose bisphosphate aldolase protein," *BioRxiv*, 2019.
- [83] A. A. Mohammed, A. M. H. ALnaby, S. M. Sabeel et al., "Epitope-based peptide vaccine against fructose-bisphosphate aldolase of *Madurella mycetomatis* using immunoinformatics approaches," *Bioinform Biol Insights*, vol. 12, p. 117793221880970, 2018.
- [84] J. S. Testa and R. Philip, "Role of T-cell epitope-based vaccine in prophylactic and therapeutic applications," *Future Virol*, vol. 7, no. 11, pp. 1077-1088, 2012.
- [85] A. Idris and M. Hassan, "Immunoinformatics predication and modelling of a cocktail of B- and T-cells epitopes from envelope glycoprotein and nucleocapsid proteins of Sin Nombre virus," *Immunome Research*, vol. 13, 2017.